

Journal of Materials Chemistry A

Accepted Manuscript



This is an *Accepted Manuscript*, which has been through the Royal Society of Chemistry peer review process and has been accepted for publication.

Accepted Manuscripts are published online shortly after acceptance, before technical editing, formatting and proof reading. Using this free service, authors can make their results available to the community, in citable form, before we publish the edited article. We will replace this *Accepted Manuscript* with the edited and formatted *Advance Article* as soon as it is available.

You can find more information about *Accepted Manuscripts* in the [Information for Authors](#).

Please note that technical editing may introduce minor changes to the text and/or graphics, which may alter content. The journal's standard [Terms & Conditions](#) and the [Ethical guidelines](#) still apply. In no event shall the Royal Society of Chemistry be held responsible for any errors or omissions in this *Accepted Manuscript* or any consequences arising from the use of any information it contains.

ARTICLE

Thermostable and nonflammable silica-polyetherimide-polyurethane nanofibrous separators for high power lithium ion batteries

Cite this: DOI: 10.1039/x0xx00000x

Yunyun Zhai,^{ab} Ke Xiao,^a Jianyong Yu,^c Jianmao Yang^d and Bin Ding^{*ac}Received 00th January 2012,
Accepted 00th January 2012

DOI: 10.1039/x0xx00000x

www.rsc.org/

Safety remains a practical concern in lithium ion batteries (LIBs), which is closely associated with the internal shorting caused by the poor dimensional thermostability at elevated temperature and the flammability of separators. Here, we report a novel strategy to fabricate thermostable and nonflammable silica-polyetherimide-polyurethane (SiO₂-PEI-PU) nanofibrous membranes via electrospinning process. Benefiting from the high porosity, interpenetrating network structure and synergetic effect of silica nanoparticles, PEI and PU, the as-prepared SiO₂-PEI-PU membranes exhibit uniform pore size distribution, high ionic conductivity (6.25 mS cm⁻¹) and good electrochemical stability up to 4.86 V. Notably, the hot oven and combustion tests reveal that the SiO₂-PEI-PU membranes possess improved thermostability displaying 2% dimensional change after exposure to 170 °C for 0.5 h and flame retardant property, which could be beneficial for improving the safety of LIBs. Significantly, the SiO₂-PEI-PU membrane based Li/LiFePO₄ cell exhibits more excellent cyclability delivering a discharge capacity of 158.91 mAh g⁻¹ at the 90th cycle and better rate capability compared with the cell based on Celgard membrane. Meanwhile, the SiO₂-PEI-PU membrane based Li/LiFePO₄ cell also shows more excellent cell performance even at elevated temperature of 60 °C. The results clearly demonstrate that the SiO₂-PEI-PU membranes are promising separator candidates, which will also pave the way for further application of nanofibrous membranes in high power LIBs.

Introduction

Safety becomes a primary concern for commercial development of high-rate and high capacity lithium ion batteries (LIBs) in hybrid electric vehicles and electric vehicles. Most of the unsafe events are closely related to the poor thermal stability of separators, which could trigger the internal shorting at elevated temperature. Among major battery components, separators not only play an important role in preventing physical contact of the cathode and anode electrodes to avoid short circuit but also serve as the electrolyte reservoir to enable the free ionic transport via liquid electrolyte-filled pores.¹⁻³ Nowadays, the commercial separators are usually made up of porous polyolefin membrane owing to their high mechanical strength, good electrochemical stability and thermal shutdown performance.² Nevertheless, the intrinsic features of polyolefin, such as poor thermal stability at high temperature (150 °C) due to the relatively low softening and melting temperature, and sluggish ionic transport caused by low porosity and poor electrolyte affinity, restrict their applications in high power LIBs.⁴ Therefore, it is highly desirable to fabricate

membranes with enhanced thermostability and high ionic conductivity to guarantee the safety and reliability of LIBs.

In an effort to solve the above-mentioned problems, electrospun nanofibrous membranes, such as polyimide,^{5,6} polyvinylidene fluoride and its copolymer,⁷⁻⁹ polymethylpentene,¹⁰ polyacrylonitrile^{11,12}, and nylon 6,6,¹³ have been extensively investigated due to their high ionic conductivity brought by high porosity and interconnected pore structure.¹⁴⁻¹⁶ Although some of these separators exhibit good dimensional thermostability, the combustion behaviors have not been studied previously. Meanwhile, there still exists some possibility of causing internal shorting and thus deteriorating battery performance due to the intrinsic large pore size of electrospun membranes. Thus, the fabrication of thermostable nanofibrous membranes with controllable pore size is still a challenging problem.

Inorganic nanoparticles like silica (SiO₂) and zirconium dioxide have been used to fabricate separators of LIBs because

they can promote ionic conductivity, thermal stability and compatibility with lithium metal.¹⁷⁻¹⁹ Polyetherimide (PEI) is an amorphous polymer with carboxyl (C=O) and oxy-ether bonds (-O-) in its molecular structure, which possesses high chemical stability, good dimensional stability and inherent flame resistance,^{20,21} thus it is a promising candidate to fabricate thermostable and nonflammable separators. Polyurethane (PU), a class of thermoplastic polymer that contains soft segments and hard segments, is used to prepare separators with high ionic conductivity because the soft segments don't form ionic cluster after being dissolved alkali metal.²² Until now, we have recently reported that hierarchical structured silica nanoparticles coated polyetherimide-polyurethane nanofibrous composite membranes are obtained by electrospinning followed by a dip-coating process.²³

In this work, we present continuous efforts to create thermostable and nonflammable SiO₂-PEI-PU nanofibrous separators with controllable pore structure via one-step electrospinning technique. Key to our development design is that the use of PEI endows the as-prepared membranes with not only improved thermostability and flame retardancy but also excellent affinity to liquid electrolyte. The SiO₂-PEI-PU membranes demonstrate high ionic conductivity, improved thermal stability and uniform pore size distribution due to the introduction of SiO₂ nanoparticles. Our work presents the feasibility of electrospun nanofibrous membranes to solve the safety problems of high power LIBs.

Experimental

Materials

Polyetherimide (PEI, Ultem 1000, Saudi Basic Industries Corporation) was purchased from Dongguan Jiangxin Plastic Co., Ltd., China. Polyurethane (PU, Elastollan 2280A10) was supplied by BASF Co., Ltd. Silica nanoparticles (SiO₂ NPs, diameter of particles, 7-40 nm, specific surface area, 120 m² g⁻¹) was obtained from Aladdin Chemistry Co. Ltd. *N,N*-dimethylformamide (DMF) was bought from Shanghai Lindi Chemical Reagents Co., Ltd., China. The Celgard 2320 membrane (Celgard, China) with a thickness of about 20 μm were used as a comparison sample. All chemicals were of analytical grade and used as received without further purification.

Fabrication of SiO₂-PEI-PU nanofibrous membranes

To prepare 7 wt% SiO₂-PEI-PU blended solutions, different amounts of SiO₂ NPs (0, 2, 5, 8, and 11 wt% based on the weight of PEI-PU) were ultrasonically dispersed into DMF for 10 min, respectively, followed by adding certain amount of PEI-PU (1/1, wt/wt) under vigorously stirring for another 12 h. The above-mentioned SiO₂-PEI-PU blended solutions were loaded into a 10 mL syringe and injected through a plastic needle with a feed rate of 1 mL h⁻¹ by using the DXES-3

spinning equipment (Shanghai Oriental Flying Nanotechnology Co., Ltd., China). A high voltage of 30 kV was applied to the needle tip, and the distance from the spinneret to an aluminum foil-covered grounded rotating collector (rotating rate of 50 rpm) was 25 cm. The ambient temperature and relative humidity were 23±2 °C and 45±3%, respectively. Then, the resulting free-standing SiO₂-PEI-PU membranes of average thickness around 50 μm were dried in a vacuum oven at 70 °C for 12 h to remove the residual solvent and transferred to a dry box for further use.

Characterization of SiO₂-PEI-PU nanofibrous membranes

The surface morphologies of relevant membranes were studied by using high resolution field-emission scanning electron microscope (FE-SEM, S-4800, Hitachi Ltd., Japan). The average pore sizes and pore size distributions of as-prepared membranes were measured by a bubble-point test using a capillary flow porosimeter (CFP-1100AI, Porous Materials Inc., USA). Porosities (*P*) of the resultant membranes were determined by using *n*-butanol uptake tests, which were calculated by the following equation:

$$P(\%) = \frac{M_{BuOH} / \rho_{BuOH}}{(M_{BuOH} / \rho_{BuOH}) + (M_m / \rho_m)} \times 100 \quad (1)$$

where M_{BuOH} and M_m are the masses of *n*-butanol and dry membranes, respectively. ρ_{BuOH} is the density of *n*-butanol, and ρ_m is the density of dry membranes, which is calculated by the composition and true density of each component. The electrolyte uptakes were investigated by the weight difference of membranes before and after soaking in a liquid electrolyte (1 M lithium hexafluorophosphate (LiPF₆) dissolved in ethylene carbonate (EC)/ethyl methyl carbonate (EMC)/dimethyl carbonate (DMC) (1/1/1, w/w/w)) for 2 h, and then calculated according to the following equation:

$$Uptake(\%) = \frac{W_w - W_d}{W_d} \times 100 \quad (2)$$

where W_d and W_w are the weights of the membranes before and after soaking electrolyte, respectively. The mechanical properties of relevant membranes were performed on a tensile tester (XQ-1C, Shanghai New Fiber Instrument Co., Ltd., China), and the bendability was measured repeatedly under longitudinal strain ranged from 10 to 30 mm at a strain rate of 10 mm min⁻¹.²⁴ Fourier transform infrared (FT-IR) spectra were recorded with a Nicolet 8700 FT-IR spectrometer in the range 4000-400 cm⁻¹. Energy-dispersive X-ray (EDX) measurements were conducted on a Philips Tecnai G2 F20 & Hitachi S-4800. Thermal shrinkages were tested by storing relevant membranes in an oven at various temperatures from 90 to 170 °C for 0.5 h, after that, dimensional changes of the membranes were carefully measured by the following equation:

$$Shrinkage(\%) = \frac{A_0 - A}{A_0} \times 100 \quad (3)$$

where, A_0 and A are the areas of relevant membranes before and after heat treatment, respectively.

Electrochemical performance evaluation

Ionic conductivity (σ) of relevant membranes was performed on liquid electrolyte-soaked membranes sandwiched between two stainless steel (SS) blocking electrodes over the frequency range from 0.1 Hz to 1 MHz with an amplitude of 5 mV by the AC impedance method using the Zahner IM 6ex impedance analyzer. The ionic conductivity could be calculated from the following equation:

$$\sigma = \frac{d}{R_b \times S} \quad (4)$$

where d is the thickness of relevant membranes, which was measured by an electronic micrometer (0.001 mm accuracy, CHY-C2 Thickness Tester, Labthink Co. Jinan, China), R_b is the bulk resistance obtained at the high frequency intercept of the Nyquist plot on the real axis, and S is the contact area between the membranes and stainless steel blocking electrode. The MacMullin number (N_m) and tortuosity (τ) of membranes can be calculated by the following equations:

$$N_m = \frac{\sigma_0}{\sigma_{eff}} \quad (5)$$

$$\tau^2 = N_m P \quad (6)$$

where, σ_0 and σ_{eff} are the ionic conductivities of liquid electrolyte (8.72 mS cm⁻¹) and liquid electrolyte soaked membranes, P is the porosity of relevant membranes. The electrochemical stability windows of the liquid electrolyte-soaked membranes were determined by linear sweep voltammetry (LSV) using a working electrode of stainless steel and counter and reference electrodes of lithium metal at a scan rate of 2 mV s⁻¹ over the potential range from 2.5 to 6.0 V vs. Li⁺/Li.

Coin cells (2016-type) were assembled by sandwiching separators between the LiFePO₄ cathode (LiFePO₄/carbon black/PVdF, 80/10/10, w/w/w) and the lithium metal anode. The mass loading of LiFePO₄ was about 8 mg cm⁻², much higher than that of most reported (about 2 mg cm⁻²). The cyclability and C-rate capabilities of the Li/LiFePO₄ cells were conducted in a Land battery test system (CT 2001A, Wuhan Land Electronic Co. Ltd., China) in a potential range of 2.5 to 4.0 V at room temperature. All the assembly processes of cells were carried out in an argon-filled glovebox with oxygen and moisture level <1 ppm.

Results and discussion

Morphology and pore structure characteristics

Fig. 1a-e show the typical FE-SEM images of the as-prepared SiO₂-PEI-PU nanofibrous membranes with various SiO₂

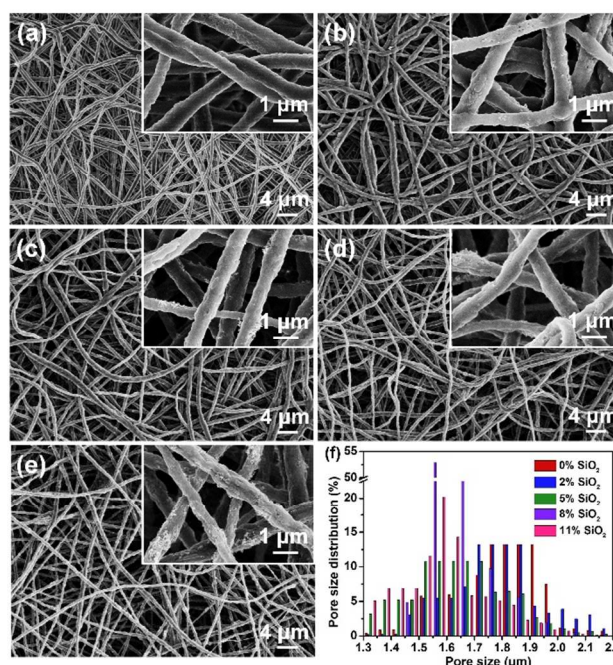


Fig. 1 FE-SEM images of as-prepared SiO₂-PEI-PU membranes containing different SiO₂ contents (a) 0 wt%, (b) 2 wt%, (c) 5 wt%, (d) 8 wt%, and (e) 11 wt%. (f) Pore size distributions of as-prepared SiO₂-PEI-PU membranes.

contents (0, 2, 5, 8, and 11 wt%). The addition of SiO₂ particles does not change the fiber diameter significantly, and all the resultant membranes exhibit tortuously interconnected porous structure constructed by randomly oriented fibers with an average diameter of 400–500 nm. But, the morphology become rougher when SiO₂ NPs are introduced (inset of Fig. 1b-e), these rough structures are generated by the wrinkles, nano protrusions formed by the SiO₂ NPs not only wrapped inside the fibers but also exposed on the fiber surface. Meanwhile, gradually increased wrinkles, nano protrusions and SiO₂ NPs are clearly visible on the fiber surface with increasing SiO₂ content, which are favorable to tune the pore structure of SiO₂-PEI-PU nanofibrous membranes. As can be seen in Fig. 1f, all the membranes have shown the pore size distributions in the range of 1.15–2.15 μm, and the average pore sizes decrease from 1.81 to 1.58 μm as the content of SiO₂ NPs increases (Table 1). It is worth noting that 77% pores of the as-prepared SiO₂-PEI-PU membranes containing 8 wt% SiO₂ NPs concentrate in the range of 1.5–1.7 μm, which confirms that SiO₂-PEI-PU membranes containing 8 wt% SiO₂ NPs possess uniform pore distribution to ensure a uniform current distribution throughout the membranes.

Porosity and electrolyte uptake

Table 1 also shows the porosities and electrolyte uptakes of Celgard membrane and as-prepared SiO₂-PEI-PU membranes with various SiO₂ content. The porosities of as-prepared membranes vary in the range of 80.66–84.97%, which are higher than the value of Celgard (49.83%) and SiO₂/nylon 6,6 membranes (70–77%).¹³ The difference in porosity could be

Table 1 Mean pore sizes, pore size distributions, porosities and electrolyte uptakes of Celgard membrane and SiO₂-PEI-PU membranes.

Samples	Mean pore size (μm)	Pore size distribution (μm)	Porosity (%)	Uptake (%)
Celgard	-	-	49.83	82.43
0 wt% SiO ₂	1.81	1.30-2.15	80.66	663.54
2 wt% SiO ₂	1.79	1.30-2.15	82.42	681.89
5 wt% SiO ₂	1.64	1.15-2.15	83.57	726.63
8 wt% SiO ₂	1.59	1.45-2.15	84.97	795.61
11 wt% SiO ₂	1.58	1.30-2.10	83.87	714.19

attributed to the difference in the porous structure and packing density of relevant membranes, as previously reported in other electrospun nanofibrous membrane system.⁹ Moreover, as shown in Table 1, the resultant SiO₂-PEI-PU membranes possess much higher electrolyte uptakes (663.54-795.61%) than Celgard (82.43%) and SiO₂/nylon 6,6 membranes (272-360%),¹³ which are consistent with the results of porosities of relevant membranes, implying that the electrolyte uptake is greatly dependent on the porosity. Meanwhile, the higher electrolyte uptakes of SiO₂-PEI-PU membranes also originate from the excellent affinity of carboxy group (PEI and PU) to carbonate ester group of liquid electrolyte.

Ionic conductivity, MacMullin number and tortuosity

It is well known that ionic conductivity is an important factor characterizing the conduction of ionic carriers. Fig. 2 presents the Nyquist plots of the electrochemical impedance for the liquid electrolyte-soaked Celgard membrane and electrospun nanofibrous membranes determined at 25 °C. The intercepts of plots on the real-axis of the liquid electrolyte-soaked membranes represent the bulk resistance. As shown in Table 2, the ionic

Table 2 Bulk resistances, ionic conductivities, MacMullin numbers and tortuosities of Celgard membrane and SiO₂-PEI-PU membranes.

Samples	Bulk resistance (Ω)	Ionic conductivity (mS cm ⁻¹)	MacMullin number	Tortuosity
Celgard	2.2	0.45	19.38	3.11
0 wt% SiO ₂	1.7	1.47	5.93	2.19
2 wt% SiO ₂	1.22	2.05	4.25	1.65
5 wt% SiO ₂	0.74	3.33	2.62	1.67
8 wt% SiO ₂	0.4	6.25	1.40	1.09
11 wt% SiO ₂	0.6	4.17	2.09	1.75

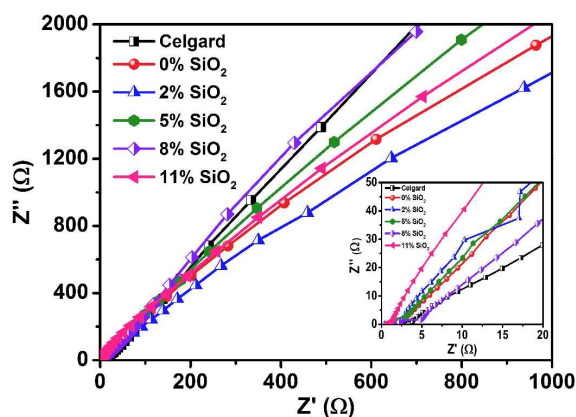
conductivities of the as-prepared SiO₂-PEI-PU membranes saturated with electrolyte vary in the range of 1.47-6.25 mS cm⁻¹, which are much higher than that of Celgard membrane (0.45 mS cm⁻¹). The higher ionic conductivity may be attributed to the higher electrolyte uptake brought by the higher porosity and the dissociation of PU to liquid electrolyte.²² Meanwhile, the Lewis acid-base interactions between the SiO₂ NPs and the electrolyte polar groups also result in an enhancement in ionic conductivity.²⁵

In addition, the MacMullin number is known to describe the deterioration of ionic conductivity because of the presence of membranes. The MacMullin numbers of SiO₂-PEI-PU membranes containing 0, 2, 5, 8, and 11 wt% SiO₂ NPs are 5.93, 4.25, 2.62, 1.40, and 2.09, respectively, which are lower than the value of Celgard membrane (19.38), indicating the lower deterioration of SiO₂-PEI-PU membranes on the battery performance. The MacMullin numbers of SiO₂-PEI-PU membranes are in accordance with their pore size, but for Celgard membrane, the value is higher than SiO₂-PEI-PU membranes because of its lower porosity although it possesses smaller pore size.²⁶

Besides, tortuosity allows taking into account the impact of the porous structure and porosity on conductivity.²⁷ The tortuosity values of resultant SiO₂-PEI-PU membranes are very close, in the range of 1.09-2.19, which are lower than the value of Celgard membrane (3.11), revealing the higher ionic conductivity of SiO₂-PEI-PU membranes from another point of view. The relatively high ionic conductivities, low MacMullin numbers and tortuosities of the SiO₂-PEI-PU membranes can be attributed to their high porosities (Table 1) with fully interconnected pore structure (Fig. 1), more electrolyte uptakes (Table 1), and good affinity of PEI and PU to carbonate solvents.

Electrochemical stability window

The electrochemical stability windows of Celgard and as-prepared SiO₂-PEI-PU membranes evaluated by LSV are shown in Fig. 3. There are no obvious increases in anodic current below

**Fig. 2** AC impedance spectra of liquid electrolyte-soaked Celgard membrane and SiO₂-PEI-PU membranes containing different SiO₂ contents at 25 °C. Inset shows the plots of high-frequency.

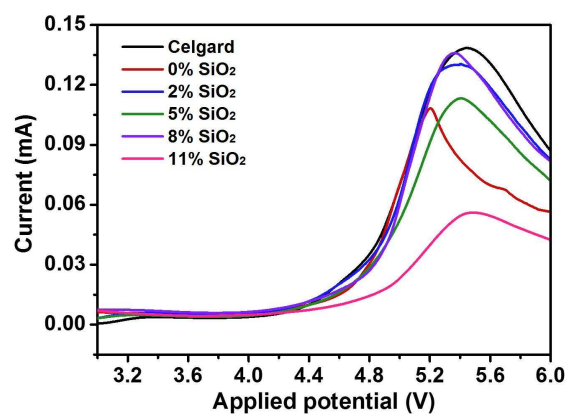


Fig. 3 Electrochemical stability windows of the cells with Celgard membrane and SiO₂-PEI-PU membranes containing different SiO₂ contents.

4.60 V for Celgard membrane, and the resultant SiO₂-PEI-PU membranes exhibit higher oxidation potentials in the range of 4.70–4.86 V, revealing that the electrochemical stabilities of SiO₂-PEI-PU membranes are high enough to be used in the high-voltage LIBs. The good electrochemical stabilities of SiO₂-PEI-PU membranes originate from the excellent affinity between the carboxy group (PEI and PU) and the carbonate ester group of liquid electrolyte.²⁸ Furthermore, the improved electrochemical stabilities are also attributed to the stabilizing effect of SiO₂ NPs, which not only absorbs some impurities such as H₂O, HF and O₂, but also reduces side reactions between the electrolyte components and the electrode.²⁹

Mechanical strength

The mechanical strength of separators should be strong enough to withstand the tension of the winding operation during battery assembly. As can be seen from Fig. 4a, the tensile strengths of as-prepared SiO₂-PEI-PU membranes gradually reduce from 8.71 to 6.22 MPa as the SiO₂ content increases, the additions of

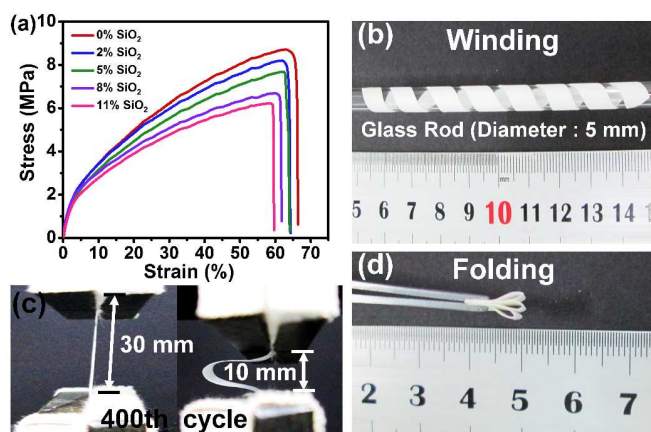


Fig. 4 (a) Stress-strain curves of as-prepared SiO₂-PEI-PU membranes. Photographs of (b) winding, (c) bending after the 400th cycle, and (d) folding tests of SiO₂-PEI-PU membranes containing 8 wt% SiO₂ NPs.

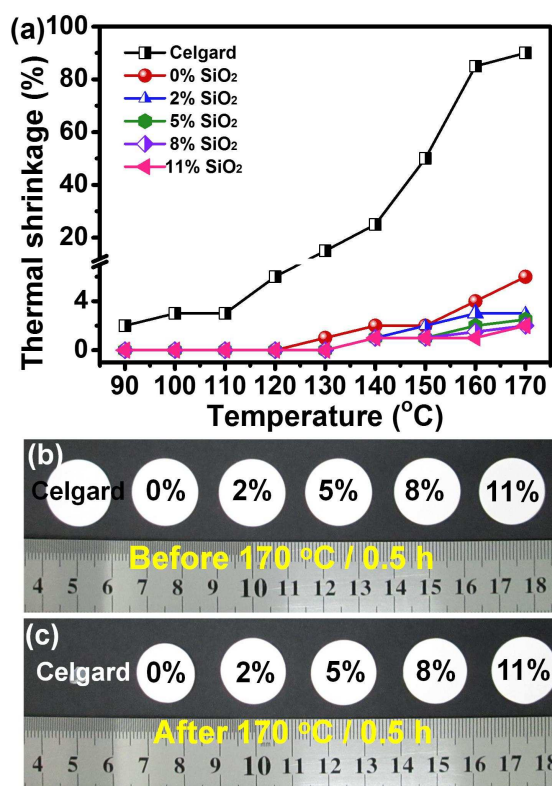


Fig. 5 (a) Comparison of thermal shrinkages of Celgard membrane and SiO₂-PEI-PU membranes as a function of heat-treatment temperature. Photographs of Celgard membrane and as-prepared SiO₂-PEI-PU membranes (b) before and (c) after exposure to 170 °C for 0.5 h.

SiO₂ NPs make the membranes slightly less flexible and thus leading to the decreases in elongation at break. The decreases of the tensile strength could be explained by the fact that the existence of wrinkles, nano protrusions and SiO₂ NPs (Fig. 1) can be served as the points of stress concentration, which become the flaws of SiO₂-PEI-PU membranes and thus deteriorating the tensile strengths. Because of the weak bonding between the loose packing nanofibers, the tensile strengths of SiO₂-PEI-PU membranes are lower than the tensile strength in both the transverse direction (12.88 MPa) and the machine direction (114.28 MPa) of Celgard membrane (Fig. S1). Despite that, the tensile strengths of SiO₂-PEI-PU membranes are still higher than those reported in the previous studies.^{10,30} Moreover, the SiO₂-PEI-PU membranes containing 8 wt% SiO₂ NPs could be severely twisted several times without breaking along a glass rod with a diameter of 5 mm (Fig. 4b), and not mechanically ruptured after being fully folded at a bending angle of almost 180° (Fig. 4d), reflecting the superior flexibility of the SiO₂-PEI-PU membranes. More notably, the SiO₂-PEI-PU membranes containing 8 wt% SiO₂ NPs can preserve their dimensional stability even after the 400th bending cycle (Fig. 4c). The above results imply that the SiO₂-PEI-PU membranes possess excellent mechanical strength, which could meet the application requirements for high-performance LIBs.

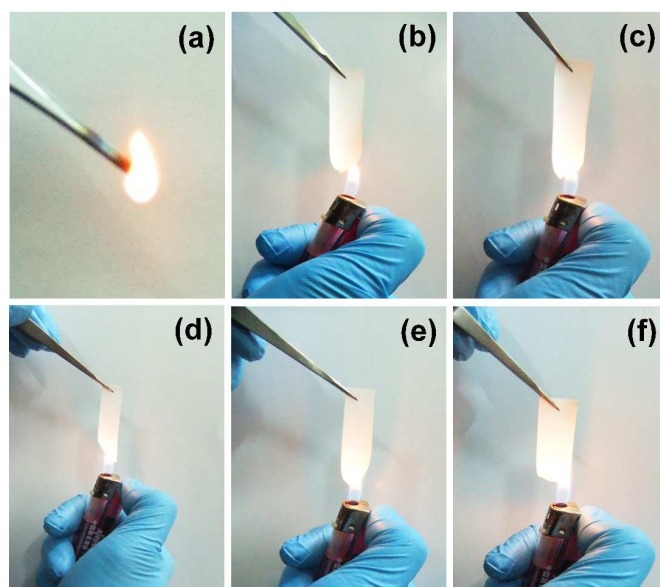


Fig. 6 Combustion tests of (a) Celgard membrane and SiO₂-PEI-PU membranes containing different SiO₂ contents (b) 0 wt%, (c) 2 wt%, (d) 5 wt%, (e) 8 wt% and (f) 11 wt%.

Dimensional thermal stability and combustion behavior

Dimensional thermal stability is one of the most significant parameters to estimate the safety characteristic of separators. As can be seen in Fig. 5a, it is noted that the Celgard membrane thermally shrinks 15%-90% as the temperature increases from 130 to 170 °C, while the dimensional changes of SiO₂-PEI-PU membranes are less than 5% except for the SiO₂-PEI-PU membranes without adding SiO₂ NPs. As presented in Fig. 5b and c, the Celgard membrane shrinks severely (90%) with the color change from white to transparent, whereas the SiO₂-PEI-PU membranes with 0 wt% SiO₂ NPs shrink by 6% and SiO₂-PEI-PU membranes with 2, 5, 8, and 11 wt% SiO₂ NPs show 2-3% thermal shrinkage at 170 °C for 0.5 h. Based on these, we can conclude that the SiO₂-PEI-PU membranes exhibit better thermal stability than Celgard membrane, which could be predominantly ascribed to the incorporation of thermotolerant PEI and SiO₂ NPs. Notably, these results demonstrate that the SiO₂-PEI-PU membranes would prevent thermal shrinkage even at elevated temperature, which is beneficial for improving the safety characteristics of LIBs.

The nonflammable property of separators is another crucial factor for the safety of LIBs, but it has been rarely mentioned because most separators are combustible, except polyimide based membrane,³¹ separator prepared using flame retardant or polymer composed of fluorine and bromine functional groups.³²⁻³⁴ The combustion tests of the Celgard and SiO₂-PEI-PU membranes are shown in Fig. 6, when Celgard is ignited, it is set on fire immediately and is completely engulfed in flame. However, the SiO₂-PEI-PU membranes exhibit perfect flame

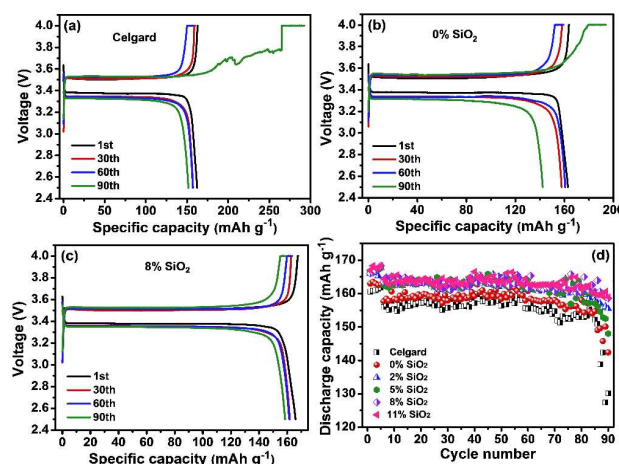


Fig. 7 Charge-discharge profiles of Li/LiFePO₄ cells assembled with (a) Celgard membrane and SiO₂-PEI-PU membranes containing (b) 0 wt% and (c) 8 wt% SiO₂ NPs. (d) Cyclability of Li/LiFePO₄ cells using Celgard membrane and SiO₂-PEI-PU membranes containing different SiO₂ contents charge-discharge at 0.2 C till 90 cycles after operating at 0.1 C for 5 cycles.

retarding ability because of the introduction of flame retarded PEI and SiO₂ NPs although they shrank. The results are in line with our previous findings indicating that SiO₂-PEI-PU membranes are promising candidates for improving the safety of LIBs.²³

Cell performance

To further evaluate the applicability of the SiO₂-PEI-PU membranes as separators for LIBs, the electrochemical behaviors of Li/LiFePO₄ coin cells incorporating the high mass loading LiFePO₄ electrode of 8 mg cm⁻² assembled with the relevant membranes and Celgard membrane were investigated. Fig. 7 illustrates the cyclability of the aforementioned coin cells charge-discharge at 0.2 C till 90 cycles after operating at 0.1 C for 5 cycles, where the coin cells are charged to 4.0 V under a constant current-constant voltage mode, and discharged to 2.5 V in a constant current mode. Fig. 7a-c show the typical charge-discharge profiles of the 1st, 30th, 60th and 90th cycle of the coin cells using Celgard membrane and SiO₂-PEI-PU membranes containing 0 wt% and 8 wt% SiO₂ NPs, respectively. All the cells exhibit a pair of flat plateaus near 3.38 and 3.5 V, and the cells using the Celgard membrane and SiO₂-PEI-PU membranes containing 0 wt% and 8 wt% SiO₂ NPs deliver initial discharge capacities of 162.25, 162.85 and 166.02 mAh g⁻¹, respectively, the results are consistent with previous reports.^{17,35} The difference in discharge capacity is probably due to the difference in the utilization of active materials, after using SiO₂-PEI-PU membranes, the porosity, electrolyte uptake and ionic conductivity increase, and hence more liquid electrolyte can diffuse from the separators to the cathode, which leads to higher utilization of LiFePO₄ active material.³⁶ However, abnormal charge behaviors are observed

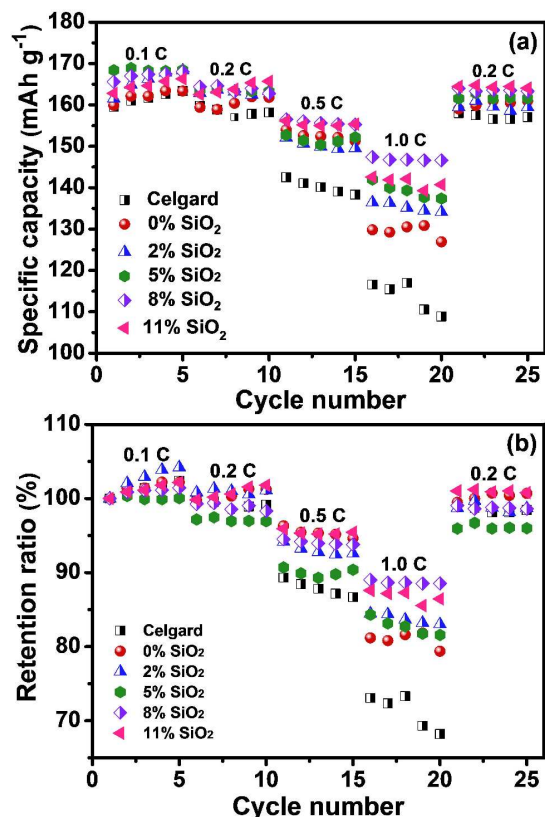


Fig. 8 (a) Comparison of discharge rate capabilities of Li/LiFePO₄ cells using Celgard membrane and SiO₂-PEI-PU membranes at different C-rate. (b) Capacity retention of Li/LiFePO₄ cells using Celgard membrane and SiO₂-PEI-PU membranes at different C-rate.

in the cells with Celgard membrane and SiO₂-PEI-PU membranes containing 0 wt% SiO₂ NPs (Fig. 7a and b), which are ascribed to the substantial increase in cell polarization caused by the use of high mass loading of cathode electrode (8 mg cm⁻²) and the slower ion transport rate during the charge-discharge reaction.²⁶ Additionally, the abnormal charge behavior may be attributed to the blocking and penetration effect caused by the dropped electrode particles and the lithium dendrite, which could trigger internal shorting and thus deteriorating battery performance.³⁷ Although, our cell using Celgard membrane demonstrates higher capacity retention (97%) after 50 cycles than those reported in the previous studies (84% and 87%, respectively).^{38,39} Moreover, the cells with the SiO₂-PEI-PU membranes exhibit more stable charge/discharge behavior compared with the cell using Celgard membrane, especially for the cells with SiO₂-PEI-PU membranes containing 8 wt% and 11 wt% SiO₂ NPs, which deliver discharge capacity of 158.61 and 158.91 mAh g⁻¹ at the 90th cycle (Fig. 7d), respectively. The improvement in cyclability of SiO₂-PEI-PU membranes may be attributed to their tortuously interconnected porous structure (Fig. 1), strong affinity of PEI and PU to liquid electrolyte (Table 2), as well as the introduction of SiO₂ NPs, as these factors could

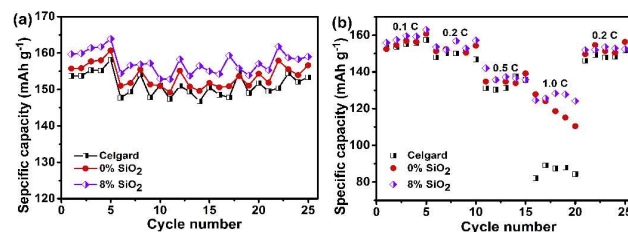


Fig. 9 (a) Cyclability and (b) rate capability of the Li/LiFePO₄ cells using Celgard membrane and SiO₂-PEI-PU membranes at elevated temperature of 60 °C.

impart more facile ion transport, higher electrolyte uptake and less adverse reactions during the cycling process.

Fig. 8 compares the discharge capacities of the cells fabricated with different membranes, with the C-rate increasing from 0.1 C to 1.0 C every 5 cycles. It is notable that the cells with SiO₂-PEI-PU membranes deliver higher discharge capacities at 0.1 C and 0.2 C, and the gaps in discharge capacities increase with increasing current density. Interestingly, when the rate returns to 0.2 C, the reversible discharge capacities of the above-mentioned cells were both close to the original capacity of 0.2 C rate, indicating that the structural stabilities of the cathode materials are retained.¹⁷ The capacity retention ratios (calculated based on the initial discharge capacity) of the cell assembled with Celgard membrane and SiO₂-PEI-PU membranes containing 0, 2, 5, 8, and 11 wt% SiO₂ NPs at the 20th cycle (1.0 C) are 68.23%, 79.38%, 81.58%, 83.03%, 88.53%, and 86.45%, respectively. The cells using SiO₂-PEI-PU membranes containing 8 wt% SiO₂ NPs exhibit better rate capability not only than the other cells using SiO₂-PEI-PU membranes but also than the cells using SiO₂/PEI-PU membranes in our previous study.²³ Notably, it seems paradoxical phenomenon that the capacity retention ratios are more than 100% at 0.1 C on occasion, which is attributed to the formation of solid electrolyte interface film during initial cycles. The improved discharge C-rate capability of the cell with SiO₂-PEI-PU membranes, especially at higher rate, can be explained by their higher ionic conductivities bring by the synergetic effect of PEI, PU and SiO₂ NPs, which reduce the concentration polarization of the electrolyte and thus delivering higher discharge capacity.

Considering the volatilization of liquid electrolyte and the thermal decomposition of LiPF₆, high temperature cell performances of the Li/LiFePO₄ cells using SiO₂-PEI-PU and Celgard membranes have been tested at 0.2 C till 25 cycles after operating at 0.1 C for 5 cycles at 60 °C. As demonstrated in Fig. 9a, the cell using the SiO₂-PEI-PU membranes containing 8 wt% SiO₂ NPs shows more stable cyclability, delivering the capacity retention of 99.6% after 25 cycles. Moreover, the cell based on the SiO₂-PEI-PU membranes containing 8 wt% SiO₂ NPs exhibits better rate capability as shown in Fig. 9b. Even at the high discharge current density (1.0 C rate), the cell exhibits a discharge capacity up to 128.3

mAh g⁻¹, which maintains 82.3% of the initial capacity at 0.1 C rate. The excellent discharge performance for the SiO₂-PEI-PU composite membranes may ascribe to the good ability to retain the electrolyte solution at high temperature. Benefiting from the good electrolyte retaining ability and the high heat resistance at elevated temperature, the SiO₂-PEI-PU membranes would enhance the safety characteristics of high power LIBs.

Conclusions

In conclusion, SiO₂-PEI-PU membranes have been successfully constructed via electrospinning technique, which has been shown to possess superior ionic conductivity and excellent safety for use in high power LIBs. Owing to the introduction of SiO₂ NPs, high porosity and electrolyte uptake, the SiO₂-PEI-PU membranes were endowed with superior ionic conductivity of 6.25 mS cm⁻¹, high anodic stability up to 4.86 V, uniform pore size distribution and improved thermostability displaying 2% dimensional change after exposure to 170 °C for 0.5 h. Notably, the Li/LiFePO₄ (high mass loading LiFePO₄ electrode of 8 mg cm⁻²) coin cells based on as-prepared SiO₂-PEI-PU membranes exhibit higher cyclability and better rate capability compared with Celgard membrane based cell not only at room temperature but also at elevated temperature, indicating that the SiO₂-PEI-PU membranes are potential separator candidates for high power LIBs. The results in this work encourage us to continue the study on high-performance LIBs with the aim of achieving high cyclability and rate capability by applying electrospun nanofibrous membranes as separators.

Acknowledgements

This work is supported by the Shanghai Committee of Science and Technology (No. 12JC1400101), the National Natural Science Foundation of China (No. 51322304), the Fundamental Research Funds for the Central Universities, and the “DHU Distinguished Young Professor Program”.

Notes and references

^a State Key Laboratory for Modification of Chemical Fibers and Polymer Materials, College of Materials Science and Engineering, Donghua University, Shanghai 201620, China. E-mail: binding@dhu.edu.cn (B. Ding)

^b College of Biological, Chemical Sciences and Engineering, Jiaying University, Jiaying 314001, China

^c Key Laboratory of Textile Science & Technology, Ministry of Education, College of Textiles, Donghua University, Shanghai 201620, China

^d Research Center for Analysis and Measurement, Donghua University, Shanghai 201620, China

† Electronic Supplementary Information (ESI) available: Stress-strain curves of the Celgard membrane, FT-IR spectra and EDX spectra of SiO₂-PEI-PU nanofibrous membranes. See DOI: 10.1039/b000000x/

- 1 P. Arora and Z. Zhang, *Chem. Rev.*, 2004, **104**, 4419.
- 2 H. Lee, M. Yanilmaz, O. Toprakci, K. Fu and X. Zhang, *Energy Environ. Sci.*, 2014, **7**, 3857.
- 3 C. M. Costa, M. M. Silva and S. Lanceros-Méndez, *RSC Adv.*, 2013, **3**, 11404.
- 4 C. J. Orendorff, T. N. Lambert, C. A. Chavez, M. Bencomo and K. R. Fenton, *Adv. Energy Mater.*, 2013, **3**, 314.
- 5 W. Chen, Y. Liu, Y. Ma and W. Yang, *J. Power Sources*, 2015, **273**, 1127.
- 6 Q. Wang, W. L. Song, L. Wang, Y. Song, Q. Shi and L. Z. Fan, *Electrochim. Acta*, 2014, **132**, 538.
- 7 W. Li, Y. Xing, Y. Wu, J. Wang, L. Chen, G. Yang and B. Tang, *Electrochim. Acta*, 2015, **151**, 289.
- 8 R. Zhou, W. Liu, J. Kong, D. Zhou, G. Ding, Y. W. Leong, P. K. Pallathadka and X. Lu, *Polymer*, 2014, **55**, 1520.
- 9 Y. Zhai, N. Wang, X. Mao, Y. Si, J. Yu, S. S. Al-Deyab, M. El-Newehy and B. Ding, *J. Mater. Chem. A*, 2014, **2**, 14511.
- 10 X. Huang, *J. Membr. Sci.*, 2014, **466**, 331.
- 11 H. Bi, G. Sui and X. Yang, *J. Power Sources*, 2014, **267**, 309.
- 12 M. Rao, X. Geng, Y. Liao, S. Hu and W. Li, *J. Membr. Sci.*, 2012, **399-400**, 37.
- 13 M. Yanilmaz, M. Dirican and X. Zhang, *Electrochim. Acta*, 2014, **133**, 501.
- 14 X. Wang, B. Ding and B. Li, *Materials Today*, 2013, **16**, 229.
- 15 X. Wang, B. Ding, G. Sun, M. Wang and J. Yu, *Prog. Mater. Sci.*, 2013, **58**, 1173.
- 16 J. Lin, X. Wang, B. Ding, J. Yu, G. Sun and M. Wang, *Crit. Rev. Solid State Mater. Sci.*, 2012, **37**, 94.
- 17 M. Raja, N. Angulakshmi, S. Thomas, T. P. Kumar and A. M. Stephan, *J. Membr. Sci.*, 2014, **471**, 103.
- 18 J. Fang, A. Kalarakis, Y. W. Lin, C. Y. Kang, M. H. Yang, C. L. Cheng, Y. Wang, E. P. Giannelis and L. D. Tsai, *Phys. Chem. Chem. Phys.*, 2011, **13**, 14457.
- 19 K. J. Kim, H. K. Kwon, M. S. Park, T. Yim, J. S. Y and Y. J. Kim, *Phys. Chem. Chem. Phys.*, 2014, **16**, 9337.
- 20 S. O. Han, W. K. Son, D. Cho, J. H. Youk and W. H. Park, *Polym. Degrad. Stabil.*, 2004, **86**, 257.
- 21 H. Fashandi and M. Karimi, *Ind. Eng. Chem. Res.*, 2013, **53**, 235.
- 22 L. Zhou, Q. Cao, B. Jing, X. Wang, X. Tang and N. Wu, *J. Power Sources*, 2014, **263**, 118.
- 23 Y. Zhai, K. Xiao, J. Yu and B. Ding, *Electrochim. Acta*, 2015, **154**, 219.
- 24 K. H. Choi, S. J. Cho, S. H. Kim, Y. H. Kwon, J. Y. Kim and S. Y. Lee, *Adv. Funct. Mater.*, 2014, **24**, 44.
- 25 Y. J. Kim, C. H. Ahn, M. B. Lee and M. S. Choi, *Mater. Chem. Phys.*, 2011, **127**, 137.
- 26 J. H. Kim, J. H. Kim, K. H. Choi, H. K. Yu, J. H. Kim, J. S. Lee and S. Y. Lee, *Nano Lett.*, 2014, **14**, 4438.
- 27 I. V. Thorat, D. E. Stephenson, N. A. Zacharias, K. Zaghib, J. N. Harb and D. R. Wheeler, *J. Power Sources*, 2009, **188**, 592.

- 28 H. R. Jung and W. J. Lee, *Electrochim. Acta*, 2011, **58**, 674
- 29 Y. Liao, C. Sun, S. Hu and W. Li, *Electrochim. Acta*, 2013, **89**, 461.
- 30 N. Angulakshmi and A. Manuel Stephan, *Electrochim. Acta*, 2014, **127**, 167.
- 31 B. Zhang, Q. Wang, J. Zhang, G. Ding, G. Xu, Z. Liu and G. Cui, *Nano Energy*, 2014, **10**, 277.
- 32 J. Zhang, L. Yue, Q. Kong, Z. Liu, X. Zhou, C. Zhang, Q. Xu, B. Zhang, G. Ding, B. Qin, Y. Duan, Q. Wang, J. Yao, G. Cui and L. Chen, *Sci. Rep-UK*, 2014, **4**, 3935.
- 33 Y. Zhu, S. Xiao, Y. Shi, Y. Yang, Y. Hou and Y. Wu, *Adv. Energy Mater.*, 2014, **4**, 1300647.
- 34 J. Woo, S. Nam, S. Seo, S. Yun, W. Kim, T. Xu and S. Moon, *Electrochem. Commun.*, 2013, **35**, 68.
- 35 J. Hao, G. Lei, Z. Li, L. Wu, Q. Xiao and L. Wang, *J. Membr. Sci.*, 2013, **428**, 11.
- 36 R. Prasanth, V. Aravindan and M. Srinivasan, *J. Power Sources*, 2012, **202**, 299.
- 37 J. Zhang, L. Yue, Q. Kong, Z. Liu, X. Zhou, C. Zhang, S. Pang, X. Wang, J. Yao and G. Cui, *J. Electrochem.Soc.*, 2013, **160**, A769.
- 38 M. Rao, X. Geng, Y. Liao, S. Hu and W. Li, *J. Membr. Sci.*, 2012, **399-400**, 37.
- 39 J. Hao, G. Lei, Z. Li, L. Wu, Q. Xiao and L. Wang, *J. Membr. Sci.*, 2013, **428**, 11.